Computers, Environment and Urban Systems 84 (2020) 101544

Contents lists available at ScienceDirect

Computers, Environment and Urban Systems

journal homepage: www.elsevier.com/locate/ceus

Sensing urban poverty: From the perspective of human perception-based greenery and open-space landscapes

Yuan Meng[a,b], Hanfa Xing[a,c,*], Yuan Yuan[d], Man Sing Wong[b], Kaixuan Fan[c]

[a] College of Geography and Environment, Shandong Normal University, Jinan, Shandong 250300, China
[b] Department of Land Surveying and Geo-Informatics, The Hong Kong Polytechnic University, 181 Chatham Road South, Kowloon, Hong Kong
[c] School of Geography, South China Normal University, Guangzhou, Guangdong 510631, China
[d] School of Geography and Planning, Guangdong Key Laboratory for Urbanization and Geo-simulation, Sun Yat-sen University, Guangzhou 510275, China

ARTICLE INFO

Keywords:
Human perception
Greenery
Open space
Landscape
Urban poverty
Street view

ABSTRACT

Greenery and open spaces play significant roles in environmentally sustainable societies, providing urban ecosystem services and economic benefits that reduce urban poverty. Current urban poverty research has solely focused on top-down observations or direct human exposure to greenery and open spaces and has failed to sense landscape characteristics, including occupation and inequality, representing the social attributes of urban poverty. This paper demonstrates the potential to better understand certain social characteristics, including occupation and inequality between urban greenery and open spaces, and to further investigate their relationship with urban poverty. Percentage and aggregation indicators are proposed based on street view images to estimate the occupation and inequality between human perception-based greenery and open spaces. The relationship between human perception and urban poverty is accordingly analysed using geographically weighted regression (GWR). The GWR model results attain an R-squared value of 0.583 and further reveal that the relationships between human perception-based landscapes and urban poverty are spatially non-stationary, indicating varying relationships across space. This implication leads to an improved understanding of the relationship between greenery and open-space landscapes and living conditions and to further allowing effective policies to help identify deprived areas.

1. Introduction

Urban poverty refers to low-level living conditions in terms of income, housing, public facilities, education and social activities and is considered one of the important issues in facilitating city organisation and decision making (Klasen, 2000; Noble, Barnes, Wright, & Roberts, 2010). Traditional approaches for measuring urban poverty are commonly based on socioeconomic situations. The use of census data and numerous urban poverty indices has been proposed, including the index of multiple deprivations (IMD) proposed by Knox and Pinch (2014), the general deprivation index (GDI) proposed by Langlois and Kitchen (2001) and the multidimensional poverty index established by Alkire and Santos (2010). These measures accurately depict socioeconomic variations to quantify urban poverty, but the impacts of the physical environment are ignored.

Remotely sensed images enable physical environment monitoring and depict the overall view of urban settlements reflecting urban poverty. On the one hand, much research has attempted to extract characteristics including colours, textures, spectra and shapes from high-resolution images to establish indicators that quantify urban poverty (Liu, Kuffer, & Persello, 2019; Wang et al., 2019). On the other hand, night-time light images, which have been suggested to be correlated with human development, have been considered to estimate economic activities and development at the local level (Bruederle & Hodler, 2018). These studies promote the determination of the spatial distribution of deprived areas from the perspective of the overall physical environment. However, few of these studies examine the configurations of specific physical elements such as greenery and open spaces and thus fail to provide detailed urban environment information to identify urban poverty settlements.

In fact, urban greenery and open spaces have long been recognised as some of the vital components in physical environmental landscapes (Kabisch & Haase, 2014; Schroeder & Cannon, 1983). Considering their contributions to the urban environment and socioeconomic conditions,

* Corresponding author at: College of Geography and Environment, Shandong Normal University, Jinan, Shandong 250300, China.
E-mail addresses: mengyuan@stu.sdnu.edu.cn (Y. Meng), xinghanfa@sdnu.edu.cn (H. Xing), yuanyuan@mail.sysu.edu.cn (Y. Yuan), Iswong@polyu.edu.hk (M.S. Wong), fankaixuan@stu.sdnu.edu.cn (K. Fan).

https://doi.org/10.1016/j.compenvurbsys.2020.101544
Received 6 April 2020; Received in revised form 7 August 2020; Accepted 10 August 2020
0198-9715/ © 2020 Elsevier Ltd. All rights reserved.

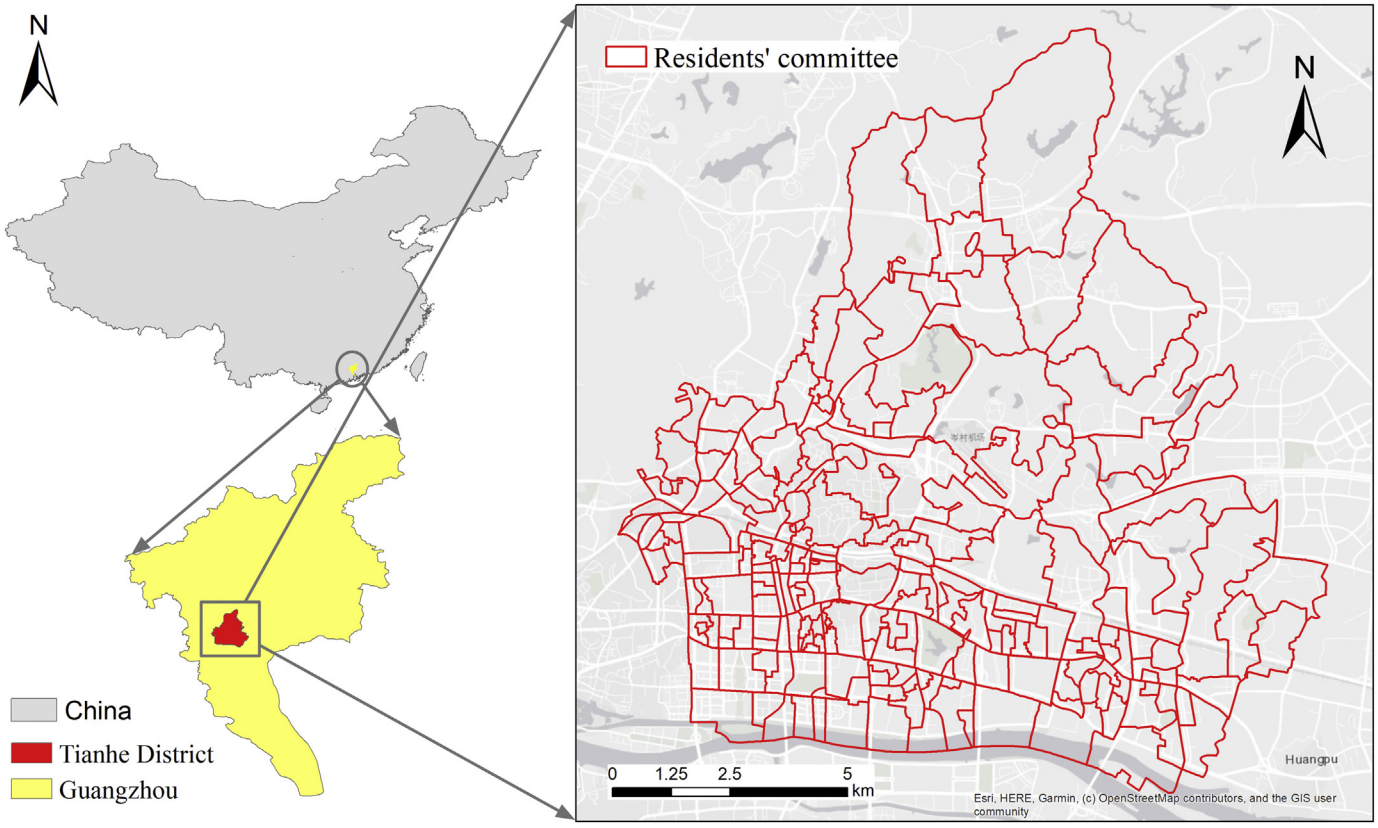


Fig. 1. Spatial distribution of the study area and street view images.

including air purification (Jim & Chen, 2008), urban heat island effect mitigation (Weng, Lu, & Schubring, 2004; Zhu, Wong, Guilbert, & Chan, 2017), urban climate investigation (Oke, 2002), urban function management (Xing & Meng, 2018; Yuen et al., 2019), physical and mental health improvement (Ho, Wong, Man, Shi, & Abbas, 2019; Lee & Maheswaran, 2011), urban crime identification (Donovan & Prestemon, 2012; Troy, Grove, & O'Neil-Dunne, 2012; Wolfe & Mennis, 2012) and sustainable development (Chen & Li, 2018), urban greenery and open spaces can potentially improve living conditions in multiple ways.

Currently, various studies have focused on the correlations between urban poverty and different perspectives of greenery or open spaces. Li et al. (2019) applied vector park data from local governments and investigated how deprived communities interact with urban greenery accessibility. Li, Zhang, Li, Kuzovkina, and Weiner (2015) utilised Google Street View (GSV) to detect the spatial distribution of residential street greenery and further analysed its relationship with the socioeconomic conditions of residents. Zhang, Zhang, Liu, and Lin (2018) employed street-level images to segment greenery and open spaces and investigate the connection between them and socioeconomic conditions. From the above research, evidence indicates that urban greenery and open spaces are significantly related to the degree of deprivation at the regional scale.

In general, physical environments are commonly depicted through remotely sensed images and vector-format local government data; ground surface boundaries, including greenery, are extracted from overhead views (Chen, Xu, & Devereux, 2014; Liu, Hu, & Li, 2017). Street view images and deep learning techniques have provided opportunities to monitor urban greenery and open spaces from vertical dimensions (Villeneuve et al., 2018; Wang, Helbich et al., 2019; Wang et al., 2018). Although street view images enable the depiction of human exposure to greenery and open spaces, state-of-the-art research mainly focuses on quantifying the visual perception of street-level landscapes (Helbich et al., 2019; Stubbings, Peskett, Rowe, & Arribas-Bel, 2019; Wang, Liu et al., 2019; Yin & Wang, 2016) and fails to depict the social attributes of greenery and open-space landscapes, including occupation and inequality. In fact, by connecting social activities and physical environments, landscape occupation conveys the sense of a containing environment from the perspective of the individual (Stenner, Church, & Bhatti, 2012), whereas landscape inequality indicates the dominant environment perceived (Wright, 2012). Compared with measuring overhead and vertical views, landscape occupation and inequality quantify integrated psycho-social-geographical environments that reflect individual living conditions. Clearly, a knowledge gap exists between the perception of greenery and open-space landscapes and urban poverty characterisation.

To overcome these constraints, this study proposes a novel framework to depict the social characteristics of urban greenery and open spaces, including occupation and inequality, and to further analyse their relationship with urban poverty. Adopting Tianhe District in Guangzhou as a case study, this research evaluates the hypothesis that perceived greenery and open spaces are represented by greenery and sky segments, respectively, in street view images (Tang & Long, 2018) and quantifies urban poverty using the modified IMD, which contains specific indications that describe living conditions (Yuan & Wu, 2014). On this basis, this study further answers the following questions:

(1) How can we effectively estimate the occupation and inequality between human perception-based greenery and open spaces reflecting the social attributes of urban poverty?
(2) Are human perception-based greenery and open spaces highly correlated with the degree of urban poverty?

The remainder of this paper is organised as follows. Section 2 introduces the study area and experimental data used in this study. Section 3 illustrates the proposed framework, including human perception-based greenery and open-space landscape descriptions and the

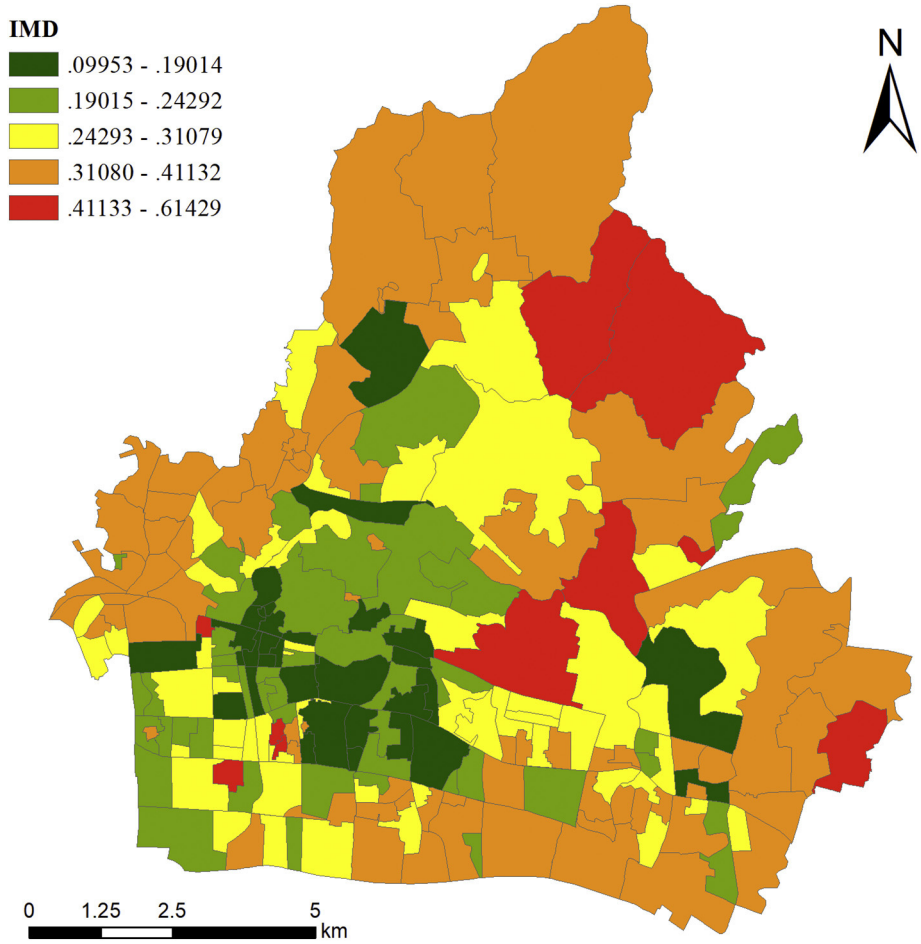


Fig. 2. Spatial distribution of the IMD for quantifying urban poverty.

analysis of the relationship of these aspects with urban poverty. In Section 4, we present the greenery, open-space landscape and quantification results and how these aspects are related to urban poverty. Section 5 analyses the contributions of human perception-based landscapes and urban poverty, examines the differences between top-down- and human perception-based landscapes and discusses the interactions between landscape occupation and inequality. Section 6 presents the conclusions of this study.

2. Study area and data

2.1. Study area

Tianhe District in Guangzhou city was selected as the study area (Fig. 1). Located in southern China, Guangzhou is the capital of Guangdong Province and one of the core cities of the Guangdong–Hong Kong–Macao Greater Bay Area. Tianhe District is the new city centre of Guangzhou and contains multiple functions to support city development. However, unbalanced development still occurs in this area. With different urban landscapes, the neighbourhoods in Tianhe range from impoverished to affluent. Thus, it is necessary to explore the variations in deprivation in Tianhe District.

2.2. Data

2.2.1. Road networks

Road networks were collected from Baidu Map (http://lbsyun.baidu.com). Roads include primary roads, secondary roads and highways, with a total length of 977.61 km. In particular, primary roads are provided for major traffic movements that connect population centres and different urban functions, whereas secondary roads are considered supplements of primary roads – typically through particular urban functions at moderate or slow speeds. Only secondary roads, with a total length of 654.25 km, were utilised because landscapes near secondary roads can be reflected in detail.

2.2.2. Street view images

Street view images were also collected from Baidu Map for data consistency ("http://quanjing.baidu.com/#/" Baidu Map, 2020). Street view locations were selected homogeneously across the road network at intervals of 100 m. Specifically, images along four headings were collected at each location, including headings of 90°, 180°, 270° and 360°. As a result, 3664 locations and 14,656 street view images were obtained. After we removed primary and highway view images, 1987 locations and 7948 street view images along secondary roads were acquired.

2.2.3. Index of multiple deprivations

The IMD is utilised to evaluate the degree of poverty. In this study, we followed the IMD in Guangzhou as calculated by Yuan and Wu (2014), who use the Fifth National Population Census of China ("http://www.stats.gov.cn/tjsj/pcsj/rkpc/dwcrkpc/" Fifth National Population Census of China, 2008) as a reference to measure urban poverty in terms of five aspects of residents' committees: income, employment, education, housing and health. Similar to a neighbourhood, residents' committees are self-organised organisations spanning several blocks in Chinese cities. In particular, 1) the evaluation of income includes the percentage of industrial workers and employees working for lower-level

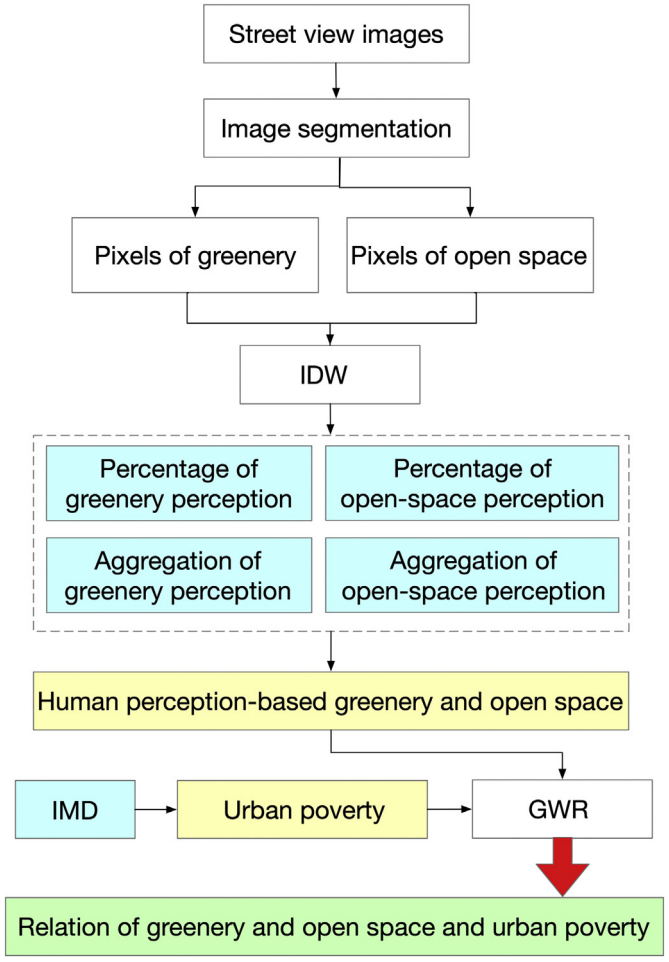


Fig. 3. Overall framework.

social services as well as the percentage of female-headed families; 2) employment indicates the percentage of unemployment over 15 years of age; 3) education includes the percentage of people between 6 and 14 years of age and not attending school, people over 15 years of age with low educational attainments and the percentage of people leaving school without a diploma; 4) housing mainly describes the percentage of households in overcrowded conditions and without clean water, showers, clean energy or toilets; and 5) health measures the ratio of disability and the percentage of people with a permanent injury, illness or physical or mental condition. As shown in Fig. 2, high IMD values represent impoverished areas, while low IMD values indicate affluent regions.

3. Methodology

3.1. Overview

In Fig. 3, an overall framework is proposed. First, image segmentation is proposed using the pyramid scene parsing network (PSPNet) (Zhao, Shi, Qi, Wang, & Jia, 2017) to extract greenery and sky segments from street view images. Then, inverse distance weighting (IDW) is applied to identify perception-based greenery and open-space landscapes from independent street view images. On this basis, four landscape indicators are established, including greenery and open-space perception percentages and aggregations. Details are provided in Section 3.2. Finally, geographically weighted regression (GWR) is utilised to analyse the relationship between human perception-based greenery and open-space landscapes and urban poverty. Details are provided in Section 3.3.

3.2. Human perception-based greenery and open-space landscape description

The descriptions of human perception-based greenery and open-space landscapes are based on two assumptions. First, the locations of street view images are considered accessible places, and thus, the views in these images are regarded as human-perceived location views. Second, indicators that describe greenery and open-space landscapes should depict continuous landscape characteristics in each residential area instead of individual street view places. Accordingly, in this section, deep learning is utilised to segment greenery and open spaces from street view images, and landscape indicators are proposed to depict greenery and open-space landscape characteristics.

3.2.1. Street view image segmentation using deep learning

Image segmentation aims to recognise independent objects and depict boundaries from a single image, which is accomplished by labelling each image pixel with a particular category. Thus, greenery and open spaces can be extracted from images by detecting greenery and sky pixels, respectively.

As shown in Fig. 4, at each location, street view images from headings of 90°, 180°, 270° and 360° are considered for human perception. Then, different objects in these street view images are automatically labelled, including buildings, sky, greenery, and cars, by applying the pyramid scene parsing network (PSPNet) architecture (Zhao et al., 2017). Model training relies on the ADE20K dataset, and this model can reach an accuracy of 79.70% for classifying 150 categories (Zhou et al., 2017).

Based on the above, greenery and open spaces are segmented from each classified street view image. Both greenery and open spaces are calculated based on pixels. Accordingly, human perception-based greenery and open spaces can be measured as follows:

$$P_{i,greenery} = \sum_{j=1}^{4} Pixel_{j,greenery} \quad (1)$$

$$P_{i,open} = \sum_{j=1}^{4} Pixel_{j,sky} \quad (2)$$

where $P_{i,\ greenery}$ and $P_{i,\ open}$ are the total pixels recognised as greenery and open spaces, respectively, at the ith location, and $P_{j,\ greenery}$ and $P_{j,\ sky}$ are the greenery and sky pixels, respectively, in the jth street view heading.

3.2.2. Greenery and open-space landscape indicators

The depiction of greenery and open-space landscapes follows the assumption that walkability is restricted to road networks; thus, human-perceived views through walkability are derived from street view images of the road network. Because perceived views outside the road networks are unavailable, they are estimated using the principle that human-perceived views close to each other exhibit notable correlations and similarities. On this basis, the IDW method, which has been applied as a means of interpolation in many fields (Bartier & Keller, 1996; F. W. Chen, 2012; Zimmerman, Pavlik, Ruggles, & Armstrong, 1999), is proposed to estimate the continuous occupation of greenery and open spaces based on the human-perceived views of street view images:

$$z_{Greenery} = \frac{\sum_{i=1}^{N} P_{i,greenery} \cdot d_i^{-n}}{\sum_{i=1}^{N} d_i^{-n}} \quad (3)$$

$$z_{Open} = \frac{\sum_{i=1}^{N} P_{i,Open} \cdot d_i^{-n}}{\sum_{i=1}^{N} d_i^{-n}} \quad (4)$$

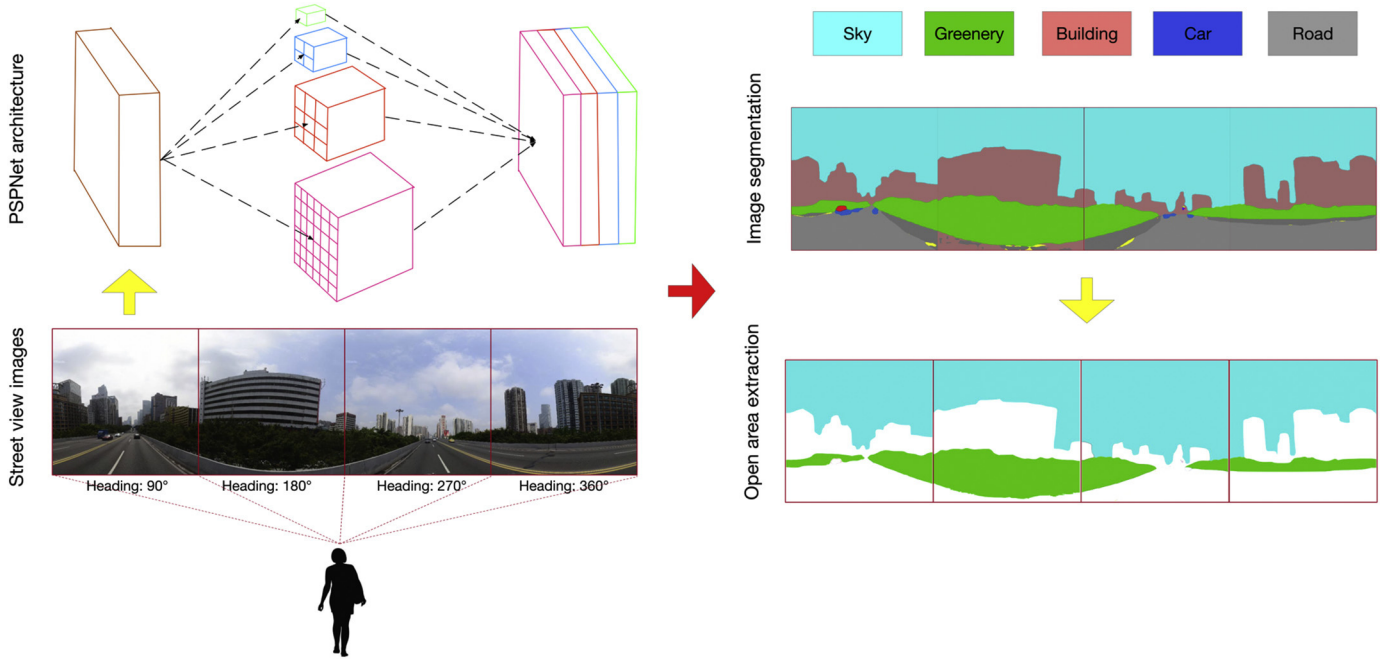


Fig. 4. The workflow of street view image segmentation for human perception.

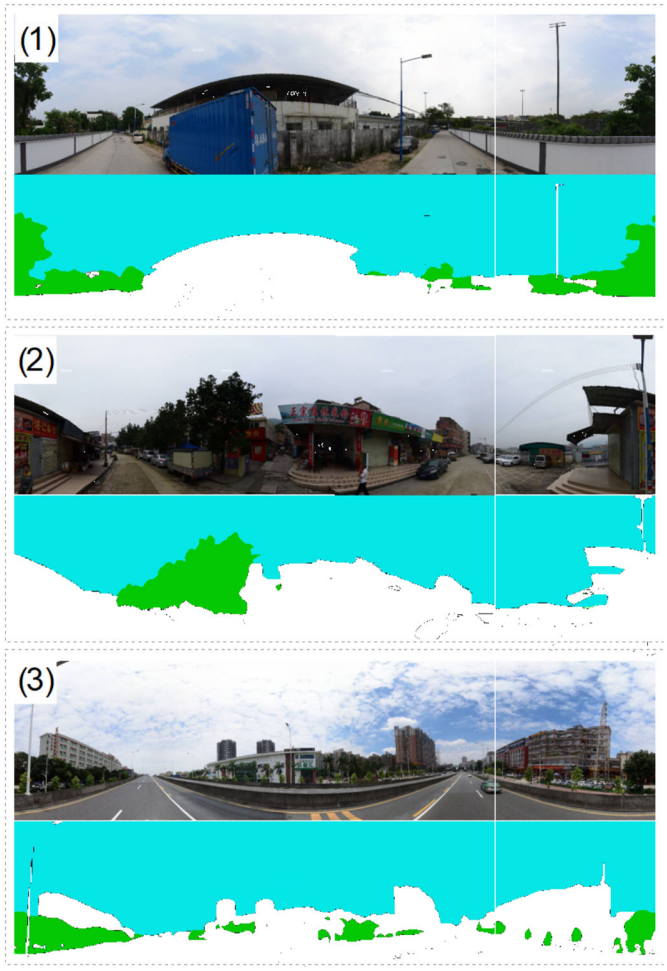


Fig. 5. Examples of greenery and open-space delineations from street view images.

where z_{Green} and z_{Open} are the estimated values of greenery and open spaces based on the ith location, d_i is the distance between the estimated and variable locations and N and n are the total locations and the coefficient to be estimated, respectively.

Based on the estimated greenery and open spaces, each area is characterised by its corresponding occupation and inequality indicators. Whereas occupation is measured by the containing percentages of greenery and open spaces, inequality is quantified by the variation in the greenery and open spaces compared with an even distribution. These indicators are modified using landscape metrics, including the percentage of the landscape and patch size standard deviation (McGarigal & Marks, 1995), and further integrate the human-centric approach in social environmental sensing (Middel, Lukasczyk, Zakrzewski, Arnold, & Maciejewski, 2019). These indicators provide an overview of human-perceived greenery and open spaces with respect to a continuous and containing landscape and further help examine how living conditions with greenery and open spaces relate to resident deprivation.

With regard to each area, the percentages of greenery and open-space perception are defined as follows:

$$Percentage_{greenery} = \frac{\sum_{i=1}^{N} z_{i,Greenery}}{\sum_{i=1}^{N} P_{i,all}} \quad (5)$$

$$Percentage_{open} = \frac{\sum_{i=1}^{N} z_{i,Open}}{\sum_{i=1}^{N} P_{i,all}} \quad (6)$$

where $P_{i,\ all}$ is calculated as:

$$P_{i,all} = \sum_{j=1}^{4} Pixel_{j,all} \quad (7)$$

where $P_{i,\ all}$ and $Pixel_{j,\ all}$ are the total pixels at the ith location and all pixels in the jth street view heading, respectively, $Percentage_{greenery}$ is the percentage of greenery perception, $Percentage_{open}$ is the percentage of open-space perception, and N is the total number of pixels within each area.

The aggregations of the greenery and open-space perception indicators are proposed as follows:

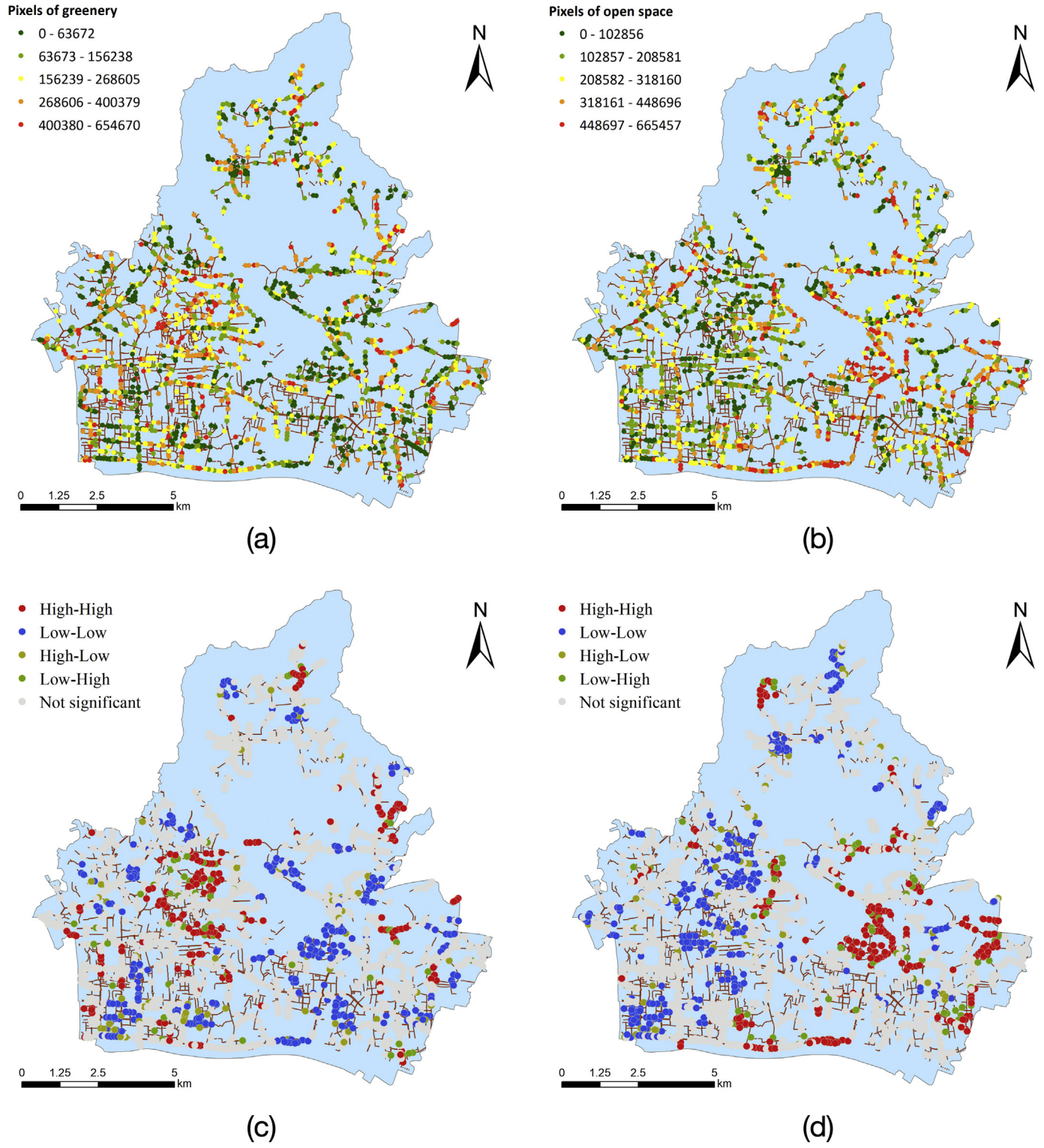


Fig. 6. Pixels in street view images to represent human perception-based greenery and open spaces and local spatial association. (a) Greenery pixels; (b) open-space pixels; (c) local spatial association for greenery; (d) local spatial association for open space.

$$Aggregation_{greenery} = \sqrt{\frac{1}{N-1}\sum_{i=1}^{N}\left(\frac{z_{i,Greenery}}{P_{i,all}} - \sum_{i=1}^{N}\frac{z_{i,Greenery}}{P_{i,all}}/N\right)^2} \quad (8)$$

$$Aggregation_{open} = \sqrt{\frac{1}{N-1}\sum_{i=1}^{N}\left(\frac{z_{i,Open}}{P_{i,all}} - \sum_{i=1}^{N}\frac{z_{i,Open}}{P_{i,all}}/N\right)^2} \quad (9)$$

where $Aggregation_{greenery}$ and $Aggregation_{Open}$ are the aggregations of greenery and open-space perception, respectively. High values indicate a high degree of inequality and variability.

3.3. Relationship analysis using GWR

To analyse the relationship between human perception-based

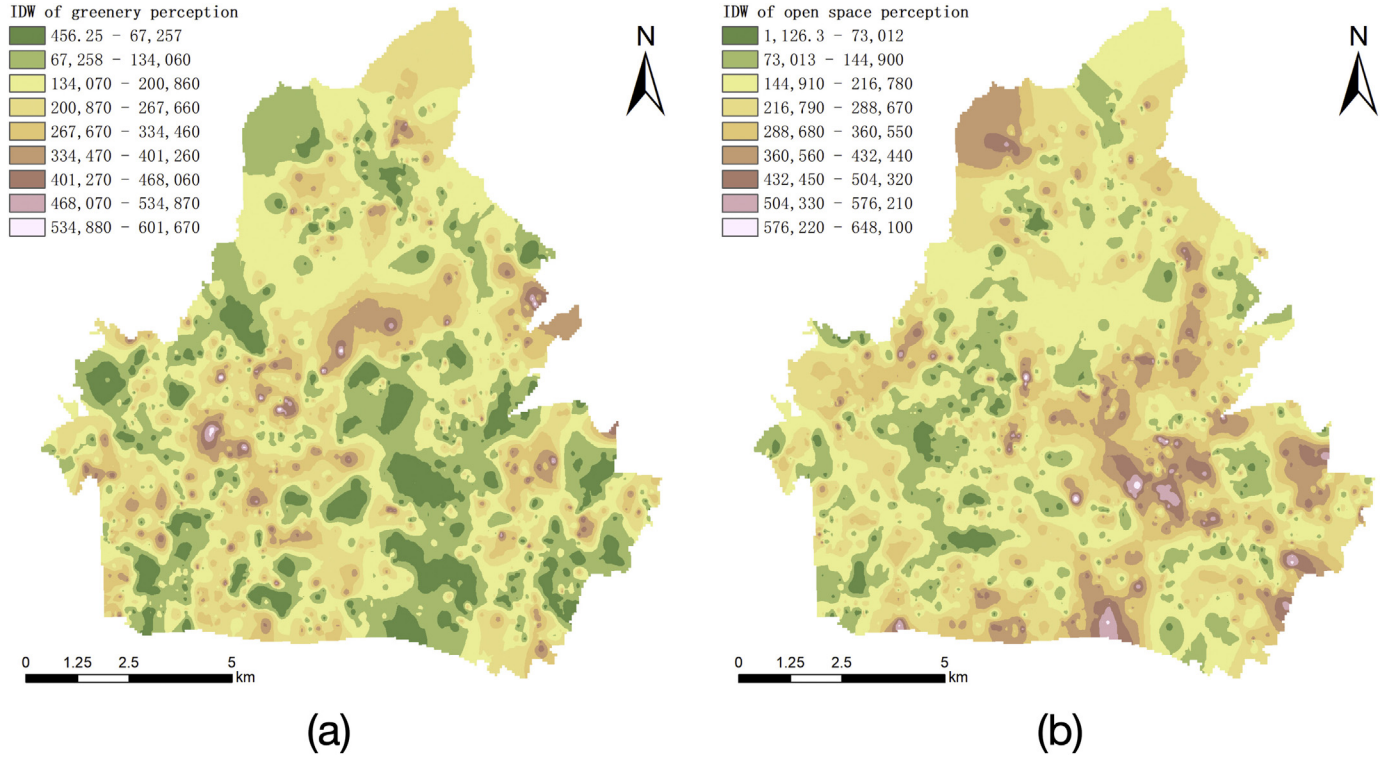


Fig. 7. Spatial distribution of the IDW results. (a) IDW greenery perception results; (b) IDW open-space perception results.

greenery and open-space landscapes and urban poverty, the GWR model, which spatially extends traditional linear regression, is applied. Compared with other spatial modelling methods, GWR is designed to analyse regressions for all locations by estimating local parameters among numerous variables (Brunsdon, Fotheringham, & Charlton, 1996). Specifically, GWR estimates a local coefficient for the *i*th location:

$$y_i = \sum_{j=0}^{j=n} \beta_{ij} * x_{ij} + \varepsilon_i \quad (10)$$

where y_i is the dependent variable at the *i*th location, x_{ij} is the independent variables, β_{ij} is the coefficient of the *j*th independent variable at the *i*th location, and ε_i is the error term. Based on the aforementioned information, indicators including greenery and open-space perception percentages and aggregations are adopted as independent variables, and the IMD quantifying urban poverty is considered the dependent variable.

In particular, the GWR model is implemented by determining the number of neighbours using the adaptive kernel. In the fitted GWR model, Akaike's Information Criterion (AICc) should be low and R-squared values should be high. In addition, GWR residuals are supposed to be randomly distributed.

In addition, to evaluate the implementation of GWR, four models, including ordinary least squares (OLS), spatial lag, spatial error, and GWR models, are evaluated. Specifically, the OLS model is assessed by spatial dependency using the Lagrange multiplier test and robust Lagrange multiplier test, and the spatial lag model and spatial error model are evaluated by spatial heterogeneity using White's test. The presence of spatial dependency and spatial heterogeneity can ensure the feasibility of the GWR model.

4. Results

4.1. Greenery and open spaces in street view images

By proposing the PSPNet architecture for image segmentation, greenery and open spaces were extracted from street view images. Fig. 5 shows the human perception-based greenery and open spaces extracted from three locations. Considering the four headings of 90°, 180°, 270° and 360°, street view images were merged to capture the surrounding environment at each location. Based on visual inspection, the proposed PSPNet model can accurately delineate the boundaries among different objects and precisely identify greenery and open spaces from street view images. In addition, there are places where the greenery is obstructed by walls and not accessible (as shown in Fig. 5(1)), and the greenery can be completely viewed in only top-down observations. A detailed discussion is provided in Section 5.

Following the delineation of greenery and open spaces, 7948 street view images at 1987 locations along secondary roads were utilised to identify greenery and open spaces. The pixels in an image of the same category (greenery or sky) at the same location were summed. Figs. 6(a) and (b) display the human perception-based greenery and open spaces at each location, respectively, and Figs. 6(c) and (d) show the local spatial association of greenery and open space. The human perception-based greenery clustered in western Tianhe District is much larger than that in eastern Tianhe District, while the human perception-based open space exhibits the opposite distribution, namely, eastern Tianhe District has more open spaces than western Tianhe District.

4.2. Human perception-based greenery and open-space landscapes

To generate continuous human perception-based greenery and open-space landscapes from the images of independent locations, both greenery and open-space pixels were considered. We determined the IDW cell size as 60 m to avoid the situation whereby each cell contained multiple street view locations and images. On this basis, the spatial distribution of the IDW greenery and open-space results are shown in

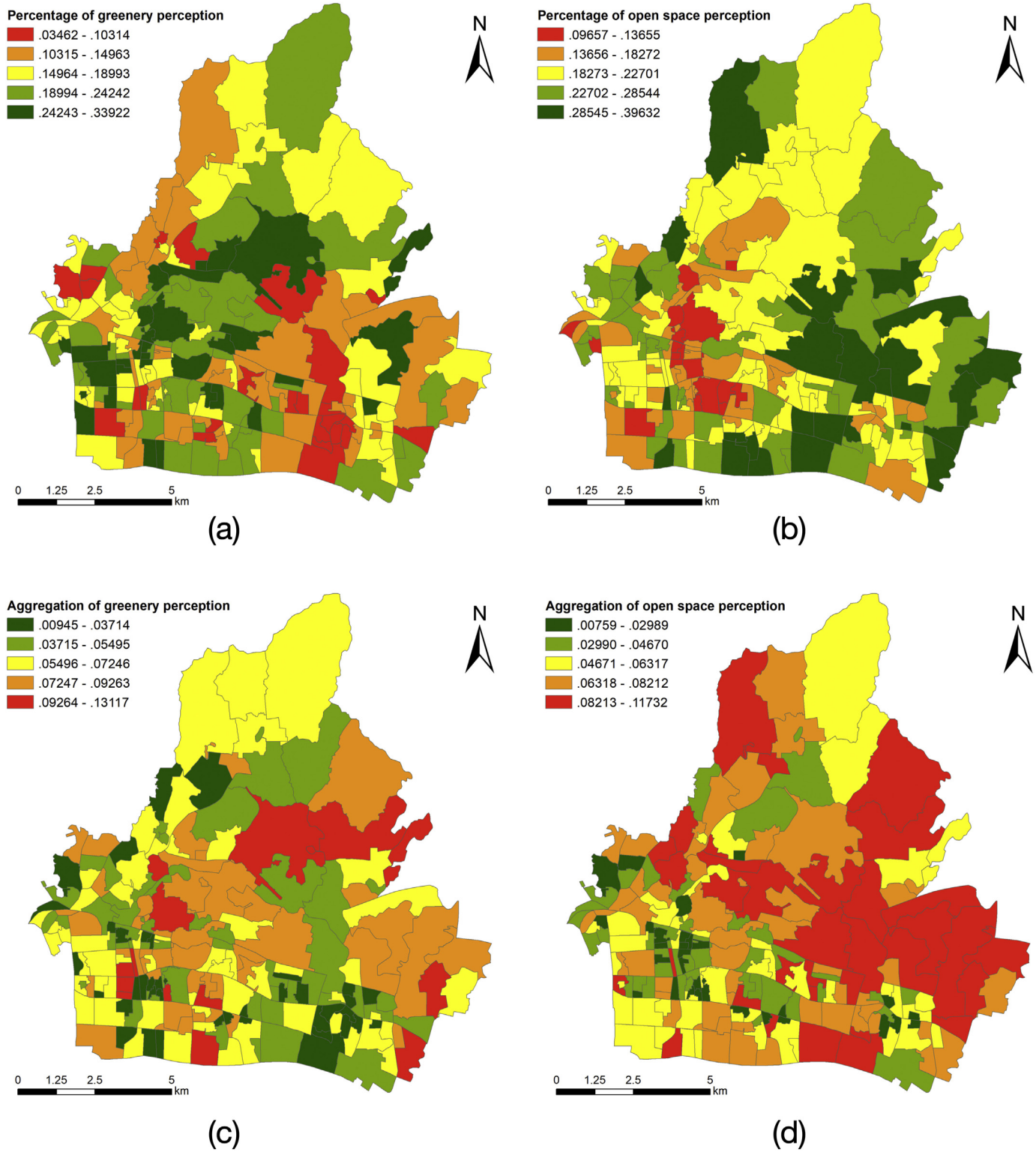


Fig. 8. Spatial distribution of human perception-based greenery and open-space landscape indicators. (a) Percentage of greenery perception; (b) percentage of open-space perception; (c) aggregation of greenery perception; (d) aggregation of open-space perception.

Fig. 7(a) and (b), respectively. These figures correspond to the visualised greenery and open spaces in Fig. 6(a) and (b), respectively, and further indicate the potential distribution of greenery and open spaces at non-image locations.

According to the continuous greenery and open-space landscapes generated via IDW, four indicators, including greenery and open-space perception percentages and aggregations, were analysed to determine the greenery and open-space landscape characteristics. Fig. 8(a)-(d) reveal that the proposed landscape indicators were calculated within each area. Both the greenery and open-space perception percentages exhibit homogeneous patterns in Tianhe District. Moreover, the distributions of both greenery and open-space perception aggregations reveal higher values in the eastern region and further indicate that East Tianhe District possesses more unequal and variable patterns of human

Table 1
Descriptive statistics of the variables.

Variable		Minimum	Maximum	Mean	Standard deviation
Independent variables	Percentage of greenery perception	0.035	0.339	0.176	0.062
	Percentage of open-space perception	0.097	0.396	0.215	0.060
	Aggregation of greenery perception	0.009	0.131	0.059	0.023
	Aggregation of open-space perception	0.008	0.117	0.057	0.024
Dependent variables	IMD	0.100	0.614	0.285	0.086

Table 2
Spatial dependency and spatial heterogeneity test.

	Lagrange multiplier test	Robust Lagrange multiplier test	White's test
OLS for spatial lag test	24.629 (P-value = 0.0000007)	9.7504 (P-value = 0.001793)	–
OLS for spatial error test	16.962 (P-value = 0.000038)	2.0842 (P-value = 0.1488)	–
Spatial lag model	–	–	28.478 (P-value = 0.0122)
Spatial error model	–	–	29.211 (P-value = 0.0098)

Table 3
Different numbers of neighbours in the GWR models and statistical results.

Number of neighbours	AICc	R-squared	Moran's I	*Z*-score	P-value
20	211.241	0.792	−0.051	−2.16	0.03
30	342.759	0.673	−0.042	−1.72	0.085
40	**385.96**	**0.583**	**−0.029**	**−1.13**	**0.26**
50	423.877	0.536	−0.015	−0.467	0.64
60	434.143	0.485	−0.002	0.152	0.879
70	438.542	0.444	0.01	0.725	0.469
80	439.541	0.409	0.022	1.255	0.209
90	439.885	0.38	0.029	1.621	0.11
100	439.858	0.356	0.036	1.92	0.055

Table 4
Comparison between OLS and GWR.

	OLS	GWR
AICc	437.48	385.96
R-squared	0.193	0.583

The bold represents the selected number of neighbours and statistical results in the implement of GWR model.

perception-based greenery and open spaces than the other regions.

4.3. Relationship between human perception-based landscapes and urban poverty

4.3.1. Model evaluation

Before the relationship between landscapes and urban poverty was modelled, descriptive statistics of both the independent and dependent variables were summarised, as shown in Table 1. In particular, the independent variables including greenery and open-space perception percentages and aggregations range between 0 and 1. The maximum greenery and open-space perception percentages are 0.339 and 0.396, respectively, whereas the minimum percentages are 0.035 and 0.097, respectively. In addition, greenery perception aggregations range from 0.009 to 0.131, whereas open-space perception aggregations vary from 0.008 to 0.117. Moreover, greenery and open spaces also exhibit similar unequal distributions among the different areas, with mean aggregations of 0.059 and 0.057, respectively.

To evaluate the feasibility of the GWR model, the spatial dependency and spatial heterogeneity of the variables were tested. As shown in Table 2, an OLS model was built, and the Lagrange multiplier values were calculated to test the spatial dependency. The Lagrange multiplier values of 24.629 (*P*-value = 0.0000007) and 16.962 (*P*-value = 0.000038) indicate that spatial dependencies exist; thus, the OLS model is not preferred to analyse the relationship between landscapes and urban poverty. Thus, spatial models, including the spatial lag and spatial error models, were proposed. Moreover, the robust Lagrange multiplier values were calculated. The results of 9.7504 (*P*-value = 0.0000007) and 2.0842 (*P*-value = 0.1488) indicate that the spatial lag model is more appropriate than the spatial error model. On this basis, the spatial heterogeneities of the spatial models were measured using White's test. The results reveal that spatial heterogeneities are significant in the spatial lag (*P*-value = 0.0122 < 0.05) and spatial error (*P*-value = 0.0098 < 0.05) models. Therefore, both OLS and spatial models are not the best approaches because of spatial dependency and spatial heterogeneity. As a result, we examined the relationship between greenery and open-space landscapes and urban poverty using the GWR model.

The GWR models with neighbour numbers that range from 20 to 100 were implemented. As shown in Table 3, the GWR models with 20, 30 and 40 neighbours attained better performance than the other models, according to AICc and R-squared values. However, the GWR model with 20 and 30 neighbours had z-scores of −2.16 and − 1.72, respectively, which are lower than −1.65, thus revealing a disperse rather than a random distribution. Thus, the GWR model with 40 neighbours was selected as the best-fitted model.

We further compared the performance of OLS and GWR. Table 4 shows that the AICc values of OLS and GWR are 437.48 and 385.96, respectively, whereas the R-squared increases from 0.193 in the OLS model to 0.583 in the GWR model, indicating that GWR is the most effective relationship modelling approach.

4.3.2. GWR results

Based on the above model evaluation, the results of GWR with 40 neighbours were summarised. Figs. 9(a)-(d) display the GWR coefficient results of the greenery and open-space perception percentages and aggregations. Specifically, the relationship between the greenery and open-space landscape indicators and IMD is spatially inconsistent. Fig. 9(a) indicates that negative trends in the correlations between greenery perception and the degree of urban poverty are observed in the northern and central areas. Fig. 9(b) reveals that the areas in the central and northern regions exhibit notably positive results. Fig. 9(c) shows that northern areas reflect positive correlations between greenery perception aggregation and the IMD. Moreover, in Fig. 9(d), positive trends between the open-space perception aggregation and the IMD are observed in the north and southwest areas, whereas positive trends are located in the eastern areas.

The local R-squared values in Fig. 10(a) indicate that the variation in greenery and open-space landscape indicators explains 0.037 to 0.632 of the variability in the IMD. In particular, the areas marked with

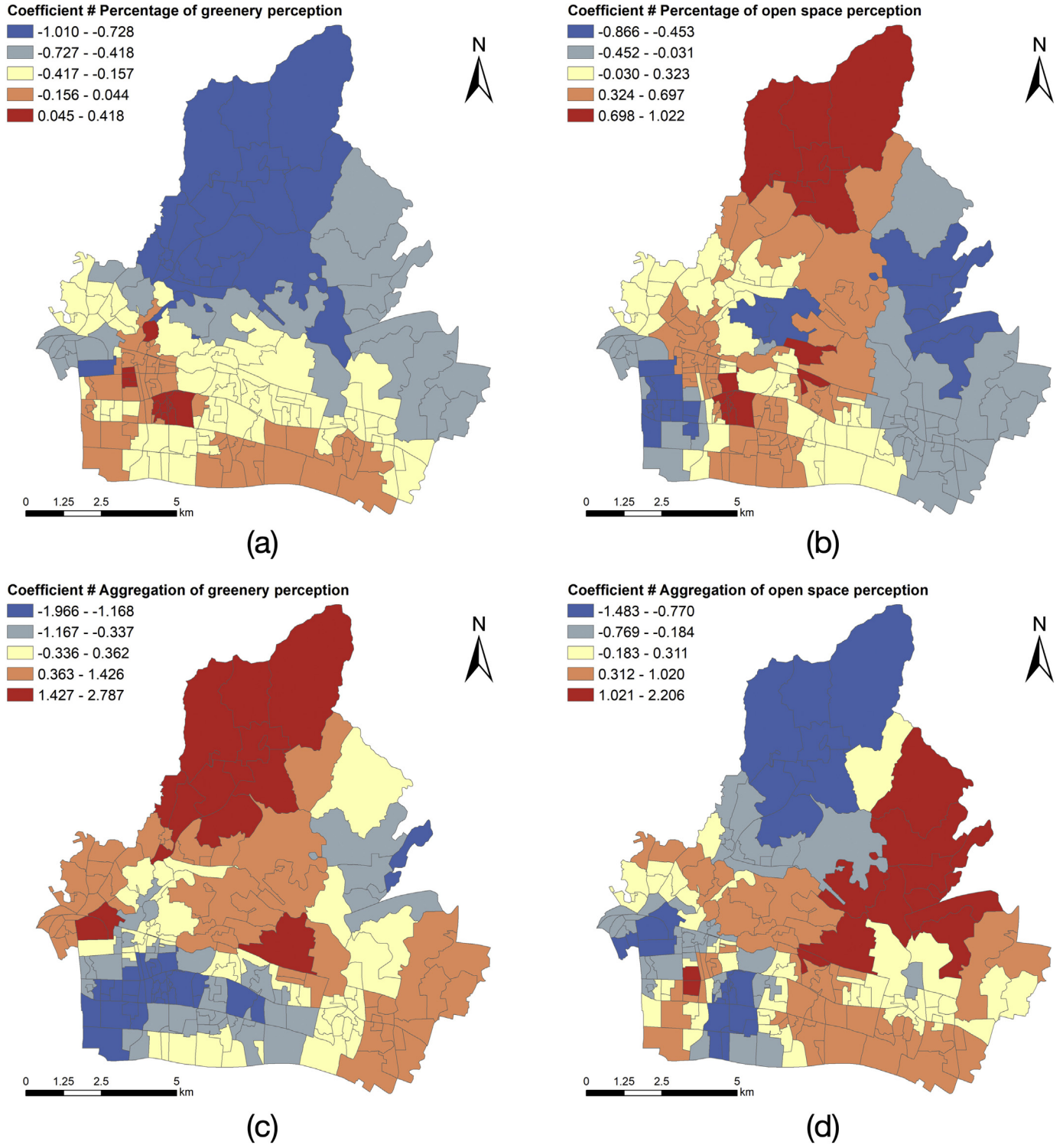


Fig. 9. GWR coefficient results. (a) Percentage of greenery perception; (b) percentage of open-space perception; (c) aggregation of greenery perception; (d) aggregation of open-space perception.

darker colours have higher local R-squared values and are mostly located in the northwest area, while the areas marked with lighter colours have lower local R-squared values and are distributed in the southeast region. Moreover, the GWR model performance is represented by the standard residuals (Fig. 10(b)), revealing any spatial correlation issues. Specifically, the standard residuals usually range from −1.96 to 1.96, that is, within the 95% confidence level. Because standard residuals in most of the areas are presented within the acceptable range, we can conclude that the GWR model is suitable for illustrating the correlation between greenery and open-space landscapes and urban poverty.

5. Discussion

5.1. Contributions of human perception-based landscapes on urban poverty

These findings suggest that human perception-based landscapes,

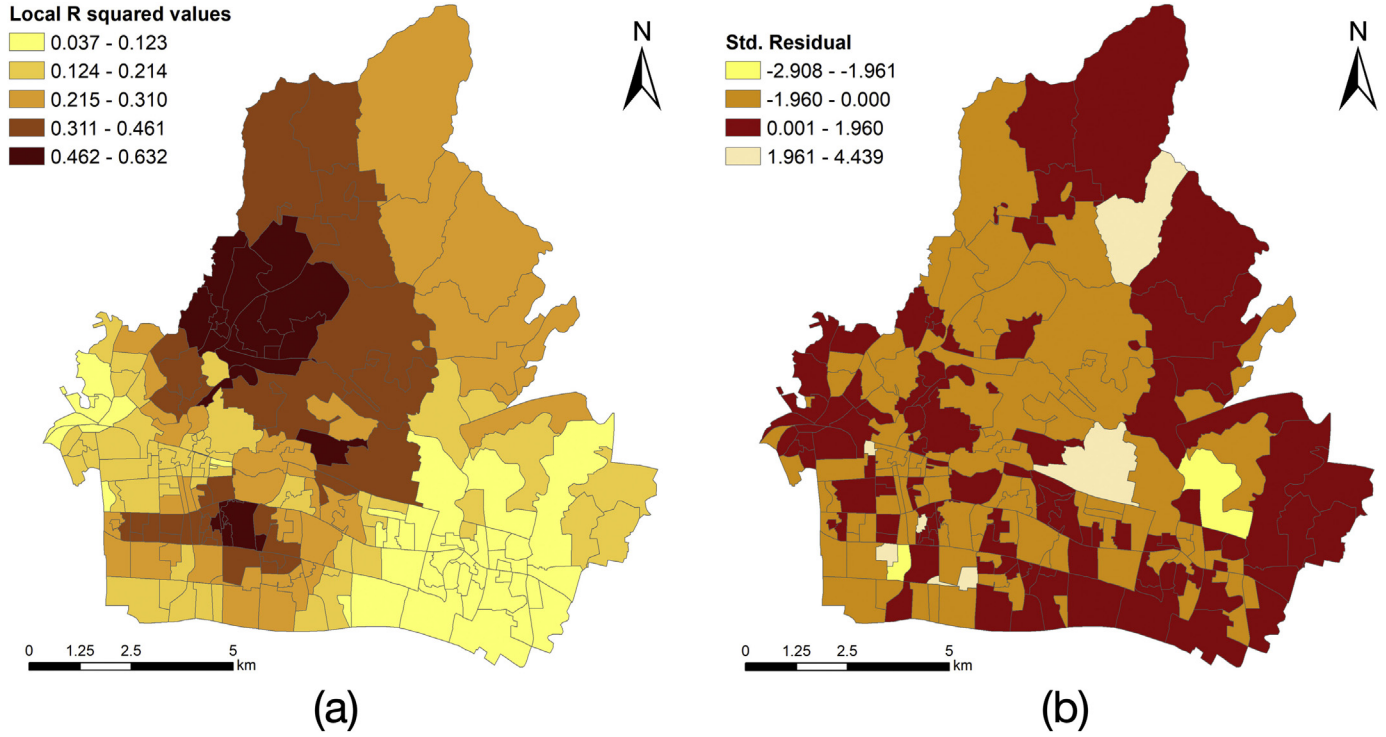


Fig. 10. GWR statistical results. (a) Local R-squared values; (b) standard residuals.

including greenery and open space, are strongly correlated with urban poverty. Compared with the OLS and spatial lag/error models, the GWR model solved the problem of spatial autocorrelation and further revealed that the relationship between human perception-based landscapes and urban poverty varies over space with different strengths (coefficients) and directions (positive/negative trends). These findings support the view that urban poverty is not only depicted by economic conditions but also reflected on environment characteristics (Niu, Chen, & Yuan, 2020).

In most areas, the percentage of greenery perception is negatively related to urban poverty, indicating that high occupation of perceived greenery is generally associated with low-level urban poverty regardless of the spatial distribution. This finding is consistent with the existing research that high-income citizens tend to live in areas with more greenery (Li et al., 2015).

A more heterogeneous pattern is found in both the strength and directions of the relationship between the percentage of open-space perception and urban poverty. Unlike greenery landscapes, the occupation of perceived open space is significantly influenced by the fraction of visible sky. The non-stationary relationship indicates that the various perceived open spaces should be investigated locally with regard to the degree of deprivation.

The relationship between the aggregation of greenery perception and urban poverty shows different directions across space. Specifically, most of the positive trends are in northern areas with high urban poverty, indicating that the unequal distribution of greenery is more likely to be perceived in more deprived areas. In contrast, Southwest Tianhe District, with much lower deprivation than other areas, shows negative trends between greenery aggregation and urban poverty.

Unlike the aggregation of greenery perception, the aggregation of open-space perception is negatively related to urban poverty in both North and Southwest Tianhe District, indicating that a more unequal perception of open space tends to reveal much lower deprivation in these areas. This result could be explained by the diversity of urban structures in multi-level socioeconomic development that leads to open-space fractions.

5.2. Comparison of top-down- and human perception-based landscapes

Top-down-based landscapes are usually depicted from satellite and airborne remote sensing images, including radiometer, radar and light detection and ranging (LiDAR) sensor images. Remote sensing views from the top-down perspective highly promote large-scale monitoring. In contrast, the availability of street view images has enabled urban landscape sensing from the perspective of human perception. Compared with top-down landscapes, human perception-based landscapes depict distinguishable urban environments from a perspective similar to that of human vision.

Before top-down- and human perception-based views are further discussed, accuracies in the depicted views should be validated. Regarding greenery landscapes, 100 samples were selected in Tianhe District using a random sampling strategy. Each sample was manually interpreted: top-down-based views were interpreted using high-resolution images in Google Earth, and human perception-based views were validated on the spot. Because human perception-based views are measured using image pixels, validation was proposed by taking photos with 360° headings from the sampled spots. The validation indicates that top-down-based views show approximately 90% accuracies, whereas pixel variations from human perception-based views are consistent with those in the samples.

When top-down- and human perception-based views depict urban structures at the same location, the landscapes from different perspectives can be notably different. Fig. 11 shows several examples of the spatial distributions of top-down-based greenery (Fig. 11(a)), human perception-based greenery (Fig. 11(b)) and the corresponding street view images and remote sensing images (Fig. 11(c)) in the study area. In particular, the locations of street view images are labelled with red markers in the remote sensing images in Fig. 11(c). In area #1, continuous large-scale greenery, in which streets are covered, can be observed from the top-down perspective. The human perception-based greenery in this area exhibits similar patterns, where high IDW values occur in Fig. 11(a), and continuous greenery is also displayed in the street view images at the same location. From this point of view, the differences in greenery between areas #2 and #3 can be determined.

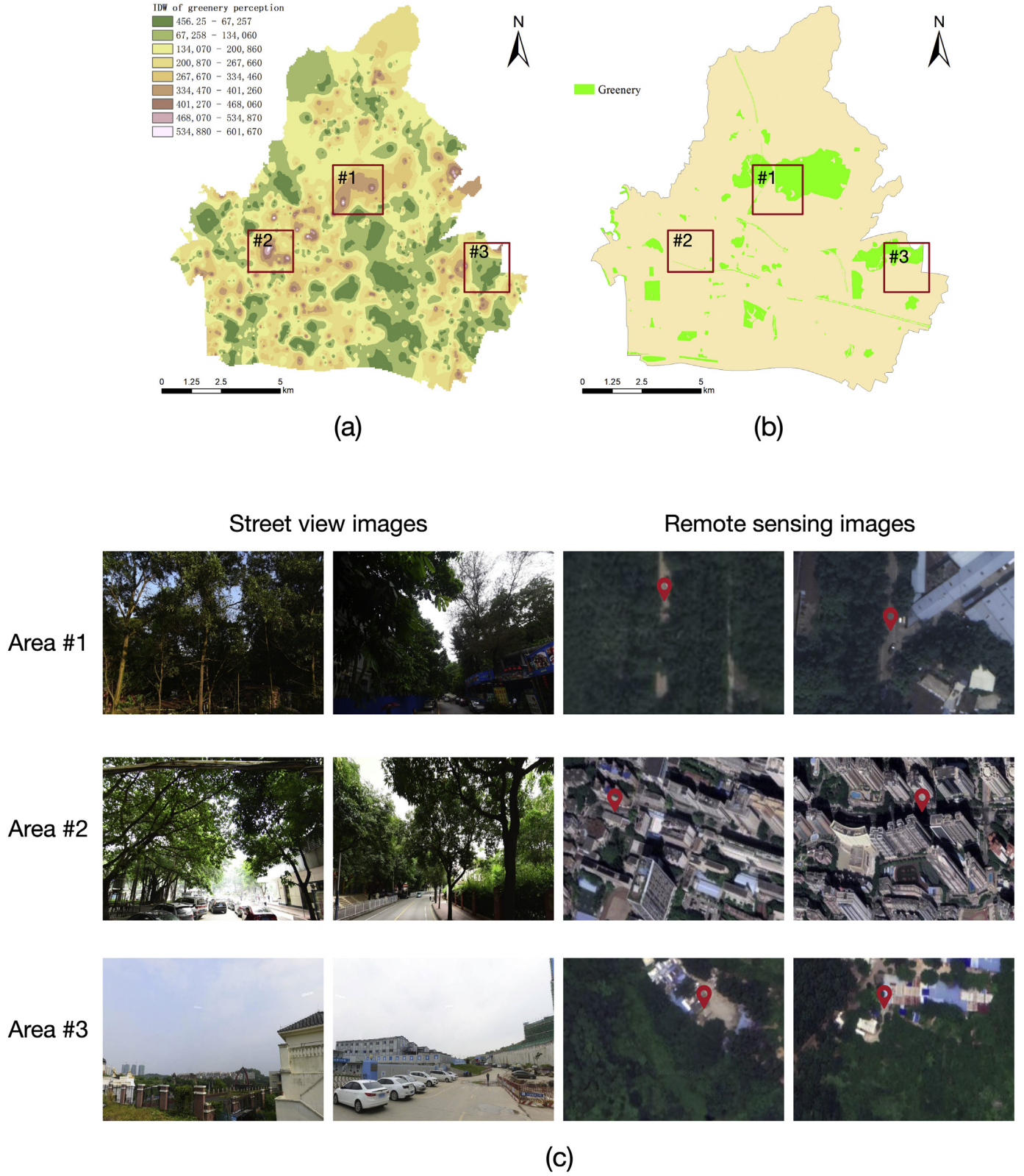


Fig. 11. Human perception- and top-down-based greenery. (a) Human perception-based greenery; (b) top-down-based greenery; (c) street view images and remote sensing images in areas #1, #2 and #3 (locations of street view images are labelled in the remote sensing images by red markers). (For interpretation of the references to colour in this figure legend, the reader is referred to the web version of this article.)

Specifically, peak IDW values in area #2 indicate extensive greenery, which is consistent with the high greenery occupation in the street view images. However, in remote sensing images, greenery such as trees is sheltered by buildings with shadows, and no significant greenery is identified in the top-down view. Another situation is depicted for area #3: although continuous greenery can be identified from a top-down perspective in the northern part, they are located away from the human-accessible areas; thus, human-perceived greenery is lacking in

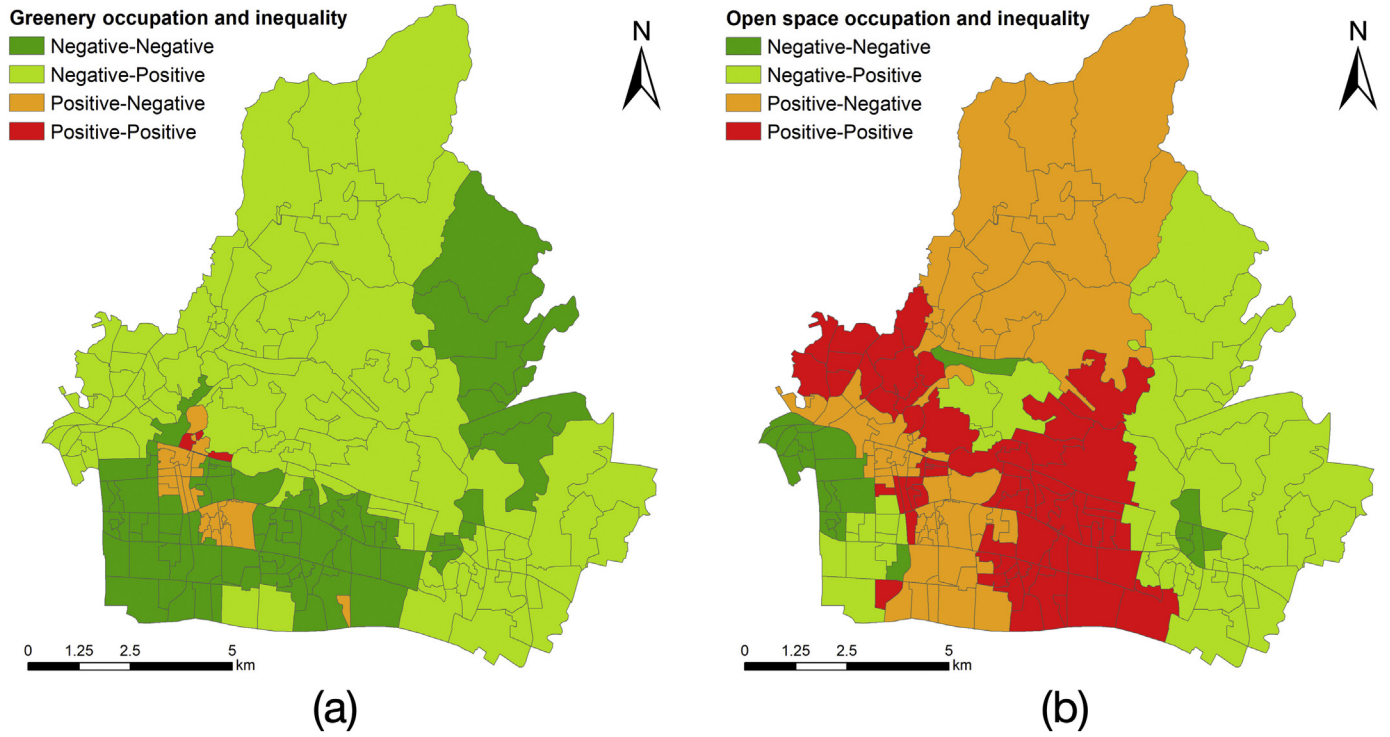


Fig. 12. Differences in occupation and inequality in response to urban poverty. (a) Greenery occupation and inequality; (b) open-space occupation and inequality.

the street view images in this area.

From this discussion, one can conclude that the spatial distributions of top-down- and human perception-based greenery are not consistent. On the one hand, more human-perceived greenery than top-down greenery was identified in certain regions, whereas on the other hand, continuous large-scale greenery from the top-down perspective cannot be completely perceived by humans. As a result, the hypothesis that urban landscapes vary according to the different perspectives is shown.

5.3. Interactions between human perception-based occupation and inequality

To gain a better understanding of human perception-based landscapes, the different impacts of occupation and inequality on urban poverty must be investigated. In particular, occupation quantifies the perceived landscapes at a global scale within an area, whereas inequality represents the variation on a local scale. For instance, positive directions of both greenery occupation and inequality on urban poverty reveal that increases in the perceived and aggregation of greenery are related to a high degree of deprivation. Thus, evaluating the consistencies and inconsistencies between the impacts of occupation and inequality provides effective insight into identifying urban poverty from a spatially heterogeneous perspective.

'Positive/Negative' patterns are proposed in Fig. 12, showing the relationship combination of 'Direction of occupation and urban poverty–Direction of inequality and urban poverty'. For greenery landscapes, Fig. 12(a) shows that, in most of the areas, greenery occupation and inequality are consistently negatively correlated with deprivation, whereas the impacts are more complex regarding open space and urban poverty. The 'Positive/Negative' patterns are distributed heterogeneously in clusters, indicating that the identification of urban poverty is highly sensitive to local conditions. Areas and neighbours could show high probabilities of having similar directions in open space–urban poverty relationships.

6. Conclusion

This study investigates greenery and open spaces from the perspective of occupation and inequality using street view images and further examines their relationship with urban poverty. To estimate the occupation and inequality, street view image segmentation and the IDW approach are applied, and four indicators, including greenery and open-space perception percentages and aggregations, are proposed. On this basis, GWR is utilised to analyse the relationship between human perception-based greenery and open-space landscapes and urban poverty. Given Tianhe District in Guangzhou as the study area, the results reveal that the relationship between human perception-based landscapes and urban poverty is spatially non-stationary, indicating that both the directions and strengths of these correlations vary across space.

These findings provide suggestions that the government and city planners should consider local conditions to identify and improve urban poverty issues. A better understanding of human perception-based landscapes could be gained based on occupation and inequality patterns to investigate local relationships. Compared with the OLS and spatial lag/error models, the utilisation of the GWR model has provided opportunities to analyse these relationships on a local scale rather than on a global scale.

Several challenges still exist. Although the relationship between human perception-based landscapes and urban poverty has been investigated, further discussions of why human perception-based landscapes are related to urban poverty should be proposed. Because urban poverty is a complex social phenomenon related to environmental and socioeconomic conditions, human perception-based landscapes can be considered as the delineation of the physical environment from a subjective perspective. In addition, future research should focus on the causality between human perception-based landscapes and urban poverty to gain a better understanding of the identification and elimination of deprivation.

Declaration of Competing Interest

The authors declare no conflict of interest.

Acknowledgments

This research was supported by the National Natural Science Foundation of China (Grant No. 41971406; 41871161); the Hong Kong Research Grants Council (Grant No. 15602619) and the Research Institute for Sustainable Urban Development, the Hong Kong Polytechnic University (Grant No. 1-BBWD).

References

Alkire, S., & Santos, M. E. (2010). Acute multidimensional poverty: A new index for developing countries. *United Nations development programme human development report office background paper*.

Baidu's Panoramic Maps (2020). http://quanjing.baidu.com/.

Bartier, P. M., & Keller, C. P. (1996). Multivariate interpolation to incorporate thematic surface data using inverse distance weighting (IDW). *Computers & Geosciences, 22*, 795–799.

Bruederle, A., & Hodler, R. (2018). Nighttime lights as a proxy for human development at the local level. *PLoS One, 13*.

Brunsdon, C., Fotheringham, A. S., & Charlton, M. E. (1996). Geographically weighted regression: A method for exploring spatial nonstationarity. *Geographical Analysis, 28*, 281–298.

Chen, F. W. (2012). Estimation of the spatial rainfall distribution using inverse distance weighting (IDW) in the middle of Taiwan. *Paddy & Water Environment, 10*, 209–222.

Chen, J., & Li, Z. (2018). China tracks its progress on SDGs. *Nature,* 184.

Chen, Z., Xu, B., & Devereux, B. (2014). Urban landscape pattern analysis based on 3D landscape models. *Applied Geography, 55*, 82–91.

Donovan, G. H., & Prestemon, J. P. (2012). The effect of trees on crime in Portland, Oregon. *Environment and Behavior, 44*, 3–30.

Fifth National Population Census of China (2008). National Bureau of Statistics of China. http://www.stats.gov.cn/tjsj/pcsj/rkpc/dwcrkpc/.

Helbich, M., Yao, Y., Liu, Y., Zhang, J., Liu, P., & Wang, R. (2019). Using deep learning to examine street view green and blue spaces and their associations with geriatric depression in Beijing, China. *Environment International, 126*, 107–117.

Ho, H. C., Wong, M. S., Man, H. Y., Shi, Y., & Abbas, S. (2019). Neighborhood-based subjective environmental vulnerability index for community health assessment: Development, validation and evaluation. *Science of the Total Environment, 654*, 1082–1090.

Jim, C. Y., & Chen, W. Y. (2008). Assessing the ecosystem service of air pollutant removal by urban trees in Guangzhou (China). *Journal of Environmental Management, 88*, 665–676.

Kabisch, N., & Haase, D. (2014). Green justice or just green? Provision of urban green spaces in Berlin, Germany. *Landscape and Urban Planning, 122*, 129–139.

Klasen, S. (2000). Measuring poverty and deprivation in South Africa. *Review of Income and Wealth, 46*, 33–58.

Knox, P., & Pinch, S. (2014). *Urban Social Geography: An Introduction.* Routledge.

Langlois, A., & Kitchen, P. (2001). Identifying and measuring dimensions of urban deprivation in Montreal: An analysis of the 1996 census data. *Urban Studies, 38*, 119–139.

Lee, A. C., & Maheswaran, R. (2011). The health benefits of urban green spaces: A review of the evidence. *Journal of Public Health, 33*, 212–222.

Li, X., Zhang, C., Li, W., Kuzovkina, Y. A., & Weiner, D. (2015). Who lives in greener neighborhoods? The distribution of street greenery and its association with residents' socioeconomic conditions in Hartford, Connecticut, USA. *Urban Forestry & Urban Greening, 14*, 751–759.

Li, Z., Wei, H., Wu, Y., Su, S., Wang, W., & Qu, C. (2019). Impact of community deprivation on urban park access over time: Understanding the relative role of contributors for urban planning. *Habitat International,* 102031.

Liu, M., Hu, Y.-M., & Li, C.-L. (2017). Landscape metrics for three-dimensional urban building pattern recognition. *Applied Geography, 87*, 66–72.

Liu, R., Kuffer, M., & Persello, C. (2019). The temporal dynamics of slums employing a CNN-based change detection approach. *Remote Sensing, 11*, 2844.

McGarigal, K., & Marks, B. J. (1995). *FRAGSTATS: Spatial pattern analysis program for quantifying landscape structure. Gen. Tech. Rep. PNW-GTR-351*US Department of Agriculture, Forest Service, Pacific Northwest Research Station.

Middel, A., Lukasczyk, J., Zakrzewski, S., Arnold, M., & Maciejewski, R. (2019). Urban form and composition of street canyons: A human-centric big data and deep learning approach. *Landscape and Urban Planning, 183*, 122–132.

Niu, T., Chen, Y., & Yuan, Y. (2020). Measuring urban poverty using multi-source data and a random forest algorithm: A case study in Guangzhou. *Sustainable Cities and Society, 102014*.

Noble, M., Barnes, H., Wright, G., & Roberts, B. (2010). Small area indices of multiple deprivation in South Africa. *Social Indicators Research, 95*, 281.

Oke, T. R. (2002). *Boundary Layer Climates.* Routledge.

Schroeder, H. W., & Cannon, W. (1983). The esthetic contribution of trees to residential streets in Ohio towns. *Journal of Arboriculture, 9*, 237–243.

Stenner, P., Church, A., & Bhatti, M. (2012). Human—Landscape relations and the occupation of space: Experiencing and expressing domestic gardens. *Environment and Planning A, 44*, 1712–1727.

Stubbings, P., Peskett, J., Rowe, F., & Arribas-Bel, D. (2019). A hierarchical urban forest index using street-level imagery and deep learning. *Remote Sensing, 11*, 1395.

Tang, J., & Long, Y. (2018). Measuring visual quality of street space and its temporal variation: Methodology and its application in the hutong area in Beijing. *Landscape and Urban Planning. 191* 103436.

Troy, A., Grove, J. M., & O'Neil-Dunne, J. (2012). The relationship between tree canopy and crime rates across an urban–rural gradient in the greater Baltimore region. *Landscape and Urban Planning, 106*, 262–270.

Villeneuve, P. J., Ysseldyk, R. L., Root, A., Ambrose, S., DiMuzio, J., Kumar, N., ... Li, X. (2018). Comparing the normalized difference vegetation index with the Google street view measure of vegetation to assess associations between greenness, walkability, recreational physical activity, and health in Ottawa, Canada. *International Journal of Environmental Research and Public Health, 15*, 1719.

Wang, J., Kuffer, M., Roy, D., & Pfeffer, K. (2019). Deprivation pockets through the lens of convolutional neural networks. *Remote Sensing of Environment, 234*, 111448.

Wang, R., Helbich, M., Yao, Y., Zhang, J., Liu, P., Yuan, Y., & Liu, Y. (2019). Urban greenery and mental wellbeing in adults: Cross-sectional mediation analyses on multiple pathways across different greenery measures. *Environmental Research, 176*, 108535.

Wang, R., Liu, Y., Lu, Y., Zhang, J., Liu, P., Yao, Y., & Grekousis, G. (2019). Perceptions of built environment and health outcomes for older Chinese in Beijing: A big data approach with street view images and deep learning technique. *Computers, Environment and Urban Systems, 78*, 101386.

Wang, W., Yang, S., He, Z., Wang, M., Zhang, J., & Zhang, W. (2018). Urban perception of commercial activeness from satellite images and streetscapes. *Companion Proceedings of the The Web Conference 2018* (pp. 647–654). .

Weng, Q., Lu, D., & Schubring, J. (2004). Estimation of land surface temperature–-vegetation abundance relationship for urban heat island studies. *Remote Sensing of Environment, 89*, 467–483.

Wolfe, M. K., & Mennis, J. (2012). Does vegetation encourage or suppress urban crime? Evidence from Philadelphia, PA. *Landscape and Urban Planning, 108*, 112–122.

Wright, J. (2012). Landscapes of inequality? A critique of monumental hierarchy in the Mongolian Bronze Age. *Asian Perspectives,* 139–163.

Xing, H., & Meng, Y. (2018). Integrating landscape metrics and socioeconomic features for urban functional region classification. *Computers, Environment and Urban Systems, 72*, 134–145.

Yin, L., & Wang, Z. (2016). Measuring visual enclosure for street walkability: Using machine learning algorithms and Google Street View imagery. *Applied Geography, 76*, 147–153.

Yuan, Y., & Wu, F. (2014). The development of the index of multiple deprivations from small-area population census in the city of Guangzhou, PRC. *Habitat International, 41*, 142–149.

Yuen, J. W., Chang, K. K., Wong, F. K., Wong, F. Y., Siu, J. Y., Ho, H., ... Yang, L. (2019). Influence of urban green space and facility accessibility on exercise and healthy diet in Hong Kong. *International Journal of Environmental Research and Public Health, 16*, 1514.

Zhang, F., Zhang, D., Liu, Y., & Lin, H. (2018). Representing place locales using scene elements. *Computers, Environment and Urban Systems, 71*, 153–164.

Zhao, H., Shi, J., Qi, X., Wang, X., & Jia, J. (2017). Pyramid scene parsing network. *Proceedings of the IEEE Conference on Computer Vision and Pattern Recognition* (pp. 2881–2890). .

Zhou, B., Zhao, H., Puig, X., Fidler, S., Barriuso, A., & Torralba, A. (2017). Scene parsing through ade20k dataset. *Proceedings of the IEEE Conference on Computer Vision and Pattern Recognition* (pp. 633–641). .

Zhu, R., Wong, M. S., Guilbert, É., & Chan, P.-W. (2017). Understanding heat patterns produced by vehicular flows in urban areas. *Scientific Reports, 7*, 16309.

Zimmerman, D., Pavlik, C., Ruggles, A., & Armstrong, M. P. (1999). An experimental comparison of ordinary and universal kriging and inverse distance weighting. *Mathematical Geology, 31*, 375–390.